

Superconducting fluctuations in the microwave conductivity of $\text{YBa}_2\text{Cu}_3\text{O}_{7-\delta}$ single crystals

I. Ukrainczyk

Department of Physics, Faculty of Science, University of Zagreb, POB 162, HR-41001 Zagreb, Croatia

A. Dulčić

Rudjer Bošković Institute, POB 1016, HR-41001 Zagreb, Croatia

and Department of Physics, Faculty of Science, University of Zagreb, POB 162, HR-41001 Zagreb, Croatia

(Received 6 September 1994; revised manuscript received 2 December 1994)

Microwave magnetoresistance was measured in a $\text{YBa}_2\text{Cu}_3\text{O}_{7-\delta}$ single crystal. The analysis of the experimental curves shows that one can distinguish between the contributions from mean-field superconductivity and fluctuations. The behavior of the former yields a mean field T_c , while the latter is used to analyze the scaling properties of the fluctuation conductivity with a predetermined T_c .

Microwave techniques have been widely used in the study of superconductors. The main advantage with respect to dc techniques is that the microwave surface resistance R_s does not vanish just below T_c , but provides valuable information on the evolution of the superconducting state as the temperature is reduced.

High- T_c superconductors have also been studied with the microwave technique.¹⁻⁶ The behavior of $R_s(T)$ in zero magnetic field was analyzed in terms of the BCS theory and two-fluid models in analogy to the studies of classical superconductors, while the role of the thermal fluctuations of the order parameter near T_c was ignored. However, high- T_c superconductors are known to exhibit strong fluctuations, as seen in measurements of specific heat,⁷ magnetization,^{8,9} and dc resistivity.¹⁰ One may expect that microwave measurements should also yield contributions due to the superconducting fluctuations,¹¹ so that the transition curve in $R_s(T)$ should not be interpreted only by the development of the mean-field superconductivity below T_c . The problem in the analysis of $R_s(T)$ is that there is no reliable criterion to determine T_c and distinguish the region dominated by fluctuations from the one where the mean-field superconductivity prevails.

In this paper, we present microwave measurements on $\text{YBa}_2\text{Cu}_3\text{O}_{7-\delta}$ single crystal, and show that magnetic field dependences of R_s at various temperatures provide additional information from where mean-field T_c can be determined unambiguously. Also, there is a marked difference between the field dependences of R_s in the mixed state and the fluctuation region. Scaling properties of the fluctuation conductivity are analyzed with the predetermined T_c .

Our measurements were made on $\text{YBa}_2\text{Cu}_3\text{O}_{7-\delta}$ single crystal ($1 \times 1 \times 0.03 \text{ mm}^3$) grown by flux method in ZrO_2 crucibles so that contamination by other elements is very low, and the quality very high.¹² The crystal was annealed in oxygen at 450°C for a total period of four weeks. The sample was mounted on a sapphire rod, which was part of a cryostat, and positioned in the center of a TE_{102} microwave cavity. The operating frequency was 9.3 GHz. The magnetic component of the microwave field was parallel to the sample surface (ab plane), while the dc magnetic field was parallel to the c axis of the crystal. The change in the surface resis-

tance R_s of the sample, induced by temperature and/or dc magnetic field variation, resulted in a change of the reflected microwave power. In order to improve the signal to noise ratio, the reflected power was pulsed in the microwave bridge (Bruker 046MRP), and a lock-in amplifier was used after the microwave detector. For calibration purposes, the sample was replaced by a copper plate of known resistivity $\rho_{\text{Cu}}(T)$. Thus, the surface resistance of the superconductor could be evaluated in absolute units (ohms).

The temperature dependence of R_s in zero dc magnetic field is shown in Fig. 1. The normal state surface resistance is given by the standard expression for skin effect in normal metals

$$R_{sn}(T) = \sqrt{\frac{\mu_0 \omega}{2\sigma_n(T)}}, \quad (1)$$

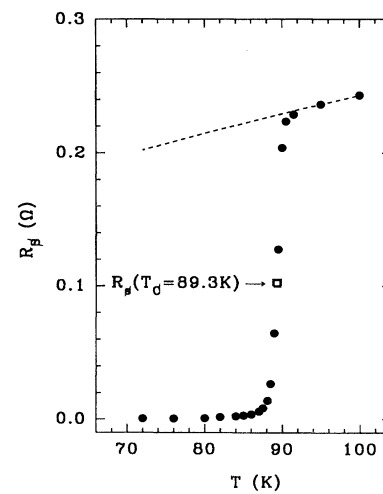


FIG. 1. Temperature dependence of the surface resistance R_s in a single-crystal $\text{YBa}_2\text{Cu}_3\text{O}_{7-\delta}$ in zero magnetic field. Dashed line shows the extrapolation of the normal state surface resistance R_{sn} . T_c denotes the mean-field critical temperature which is determined from magnetic field dependences of R_s .

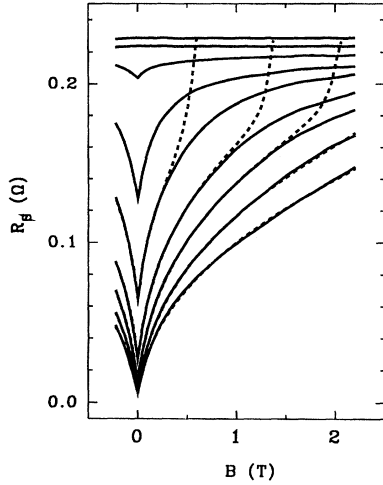


FIG. 2. Experimental magnetic field dependences of R_s (solid lines) in a single-crystal $\text{YBa}_2\text{Cu}_3\text{O}_{7-\delta}$ at various temperatures (from top to bottom: 91.5, 90.5, 90, 89.5, 89, 88.5, 88.1, 87.5, and 87 K). Dashed lines show the theoretical behavior of R_s in the mixed state. The deviation of the experimental curves from the mixed state behavior is due to the superconducting fluctuations.

where μ_0 is the permeability of vacuum, $\omega/2\pi$ is the microwave frequency, and $\sigma_n(T)$ is the normal state conductivity. R_{sn} was measured up to 120 K (not shown in Fig. 1), and the data were used to determine linear resistivity $\rho_n(T) = (0.018T - 0.17) \mu\Omega \text{ m}$.¹³ Using this $\rho_n(T)$ one may calculate from Eq. (1) the extrapolation of the normal state surface resistance which is shown by the dashed line in Fig. 1. The deviation of the measured R_s from the extrapolated $R_{sn}(T)$ becomes appreciable at temperatures below 95 K.

The transition curve in Fig. 1 is smooth and sharp, which is a clear sign of the high quality and homogeneity of the sample.¹⁴ There is, however, some rounding at the onset of the transition, which was not analyzed in the previous reports,^{1-6,14} and might cast some doubt on remaining inhomogeneities. In the present paper, we show by a detailed analysis of the magnetic field dependences of R_s that the rounding at the onset of the transition curve is due to the fluctuations of the order parameter. This analysis also yields the mean-field transition temperature $T_c = 89.3$ K in an unambiguous way. We note that in the previous reports,¹⁻⁶ T_c could not be determined by a physically solid criterion, and was usually placed somewhere at the apparent onset. In contrast Fig. 1 shows that more than half of the transition in $R_s(T)$ occurs above the mean-field T_c due to the superconducting fluctuations.

The magnetic field dependence of the surface resistance gives an additional dimension for analysis. In Fig. 2 we show the experimental curves (solid lines) at various temperatures. The normal state is characterized by the lack of any field dependence of R_s . As the temperature is reduced, the superconductivity brings in a marked field dependence. The shapes of the experimental curves are different from those observed by Owliaei, Sridhar, and Talvacchio¹⁵ in thin films. We note that the thickness of our single crystal exceeds the normal state microwave skin depth, and *à fortiori* the penetration depth in the superconducting state. In thin films, on

the contrary, the penetration depth may cross the film thickness due to temperature and/or field variations, and the experimental curves may take different forms.

Well below the superconducting transition, the role of fluctuations is expected to become negligible. Hence, we may analyze the low-temperature curves in Fig. 2 in terms of the mixed state. Note that due to the geometrical factor of the sample, the flux penetration starts at very low applied fields. Also, one can use the approximation $B \approx \mu_0 H_a$, where H_a is the applied field. On the other hand, demagnetizing effects for the microwave magnetic field are avoided by the choice of its polarization along the plane of the sample. The surface resistance in the mixed state is given by

$$R_s = \text{Re}(Z_s) = \text{Re} \sqrt{i \frac{\mu_0 \omega}{\tilde{\sigma}_v}}, \quad (2)$$

where Z_s is the complex surface impedance and $\tilde{\sigma}_v$ is the effective microwave conductivity in the mixed state. $\tilde{\sigma}_v$ involves the combined response to microwaves by the superconducting medium outside the vortex cores, and the oscillating vortices. The microwave current flows in the ab plane and along the c axis. The latter contribution to R_s can be neglected in view of the small sample thickness, and the absence of the Lorentz force on the vortices. For the microwave current perpendicular to the flux lines, we have recently found the expression¹⁶

$$\frac{1}{\tilde{\sigma}_v} = \frac{1 - b(v/v_f)}{(1 - b)\sigma + b\sigma_n} + \frac{b}{\sigma_n} \frac{v}{v_f}, \quad (3)$$

where $b = B/B_{c2}$ is the reduced field, $\sigma = \sigma_1 - i\sigma_2$ is the Meissner state microwave conductivity, and v/v_f is the ratio of the vortex velocity and the flux flow velocity in the microwave driven oscillations. This ratio is close to unity. A small deviation will be discussed below. The temperature dependence of $\tilde{\sigma}_v$ and R_s comes from $\sigma(T)$, while the field dependence is explicitly given by b in Eq. (3). One may try to fit the experimental curves in Fig. 2 by the expressions (2) and (3). The experimental value of R_s at zero field puts a constraint on σ_1 and σ_2 at a given temperature, so that only one of them is an independent parameter. Thus, the fit parameters are σ_1 (or σ_2) and B_{c2} for each curve. Note that σ_1 enters only the first term in Eq. (3). We found that this term was dominant only for very small b values, so that the choice of σ_1 was not crucial, and the curves in Fig. 2 were mainly fitted by the choice of B_{c2} . At low temperatures, the theoretical curve fits the experimental one over the whole range 0–2.25 T in Fig. 2. However, at temperatures above 87.5 K, the attempts to fit the entire curve become unsuccessful. This can be explained in the following way. When the field is increased so that it gets close to B_{c2} , the fluctuations become very strong, and the system is no longer in the mixed state. Hence, Eqs. (2) and (3) should be used to fit only some low field segments of the high-temperature experimental curves in Fig. 2. The boundary can be determined by considering the temperature dependence of R_s at a given field B . At large fields, the second term in Eq. (3) dominates. Assuming a linear Ginzburg-Landau dependence for $B_{c2}(T)$, one can plot the experimental R_s versus $(1 - t)^{-1/2}$, where $t = T/T_c$ is the reduced temperature, and

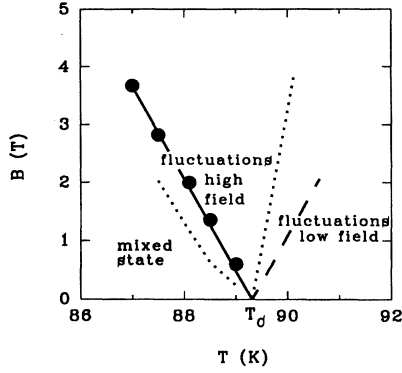


FIG. 3. Field-temperature diagram in a single-crystal $\text{YBa}_2\text{Cu}_3\text{O}_{7-\delta}$. The full circles represent B_{c2} values determined from the mixed state behavior in Fig. 2. The dashed line marks \bar{B}_{c2} at $T > T_c$, which is symmetric to B_{c2} . The dotted lines separate the regimes of mixed state, high field fluctuations, and low field fluctuations (see text).

find the point at which the experimental data start to deviate from the theoretical line for the mixed state. Thus, we determine the region where the superconductor is well in the mixed state. The fits to the appropriate low field segments of the experimental curves in Fig. 2 are found to be good. All the fits are shown by the dashed lines in Fig. 2. Here we allowed a small deviation of v/v_f from unity, which is needed for an almost perfect fit. Namely, the ratio v/v_f can be expressed as¹⁶

$$\frac{v}{v_f} = \frac{1 + i(\omega_0/\omega)}{1 + (\omega_0/\omega)^2}, \quad (4)$$

where the characteristic frequency ω_0 depends on the pinning potential and vortex lattice elasticity, both of which have some field dependence. We found a good agreement with the form $(\omega_0/\omega) = pb^\alpha$. The fits were the best with $p \approx 0.4$, and $\alpha \approx 0.4$. Once the fit parameters for a given temperature are found, the theoretical curve can be drawn beyond the experimental segment used for fitting. It reaches the normal state R_{sn} at B_{c2} . If the fluctuations were orders of magnitude weaker, the experimental curve would follow the

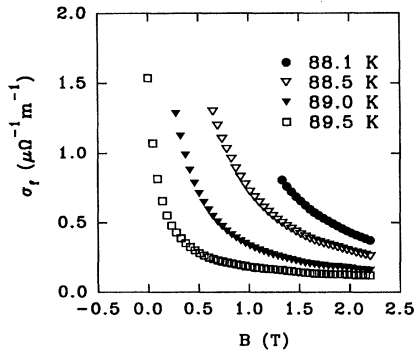


FIG. 4. Field dependences of the excess fluctuation conductivity at various temperatures. The upper three temperatures are below the mean-field T_c , while the bottom temperature is above T_c .

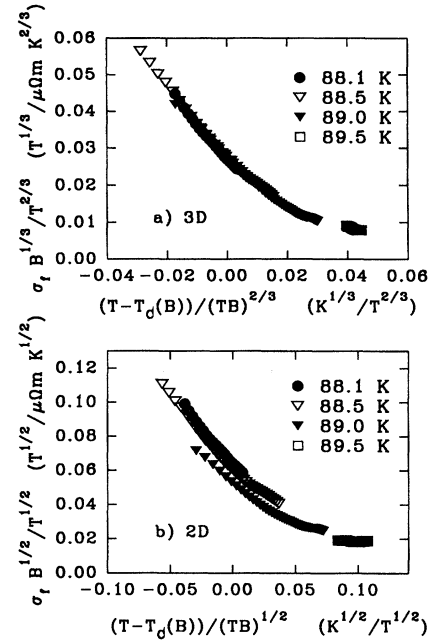


FIG. 5. Scaling of the excess fluctuation conductivity σ_f in the high field regime. The mean-field T_c is predetermined from B_{c2} in Fig. 3, so that the scaling is performed with no free parameters. 3D scaling is very good (a), while 2D scaling does not agree with the experimental data.

mixed state behavior with the upturn just below B_{c2} . This was observed, e.g., in classical superconductors.¹⁷ In the present case where the fluctuations are strong, B_{c2} is not the field at which the normal state is reached. The meaning of B_{c2} should be found within the mean-field superconductivity where the coherence length is $\xi = (\Phi_0/2\pi B_{c2})^{1/2}$, where Φ_0 is the flux quantum. Thus, when B_{c2} is ascribed to a given experimental curve in Fig. 2, it means that the vortices in the mixed state regime have a corresponding radius ξ . The number of vortices increases with the field, but at a given temperature their radius remains the same. When the applied field approaches the value of B_{c2} , the mixed state becomes overwhelmed by strong fluctuations, so that R_s does not reach the normal state value.

The values of B_{c2} obtained from the fits are shown in Fig. 3. The data points lie on a straight line with slope -1.7 T/K. Similar slopes were obtained by Welp *et al.* from magnetization measurements.⁸ The mean-field critical temperature T_c is characterized by the divergence of ξ , which implies also the vanishing of B_{c2} . From the extrapolation of the solid line in Fig. 3, we get $T_c = 89.3$ K. This is the temperature indicated in Fig. 1. At low temperatures, the experimental lines do not reach B_{c2} . At temperatures closer to T_c , one observes that at some field a transition occurs from the mixed state into the fluctuation regime. The dotted line at $T < T_c$ in Fig. 3 marks the crossover as seen from the deviation of the experimental curves in Fig. 2 from the theoretical lines for the mixed state. At temperatures higher than T_c , the experimental lines are entirely in the fluctuation region.

The surface resistance in the fluctuation region is given by

$$R_{sf}(T) = \sqrt{\frac{\mu_0 \omega}{2(\sigma_n + \sigma_f)}}, \quad (5)$$

where σ_f is the excess fluctuation conductivity. From the experimental curves in Fig. 2, and the values of $\sigma_n(T)$ determined from Fig. 1, one can deduce the excess fluctuation conductivity σ_f . Figure 4 shows σ_f as a function of the magnetic field at various temperatures. It is interesting to examine scaling laws for σ_f . Ullah and Dorsey¹⁸ analyzed the scaling behavior in high magnetic fields within the Hartree approximation for the interactions between the fluctuations. For $T < T_c$, they predict that the fluctuations merge into mean-field superconductivity when the field is reduced somewhat below B_{c2} . For $T > T_c$, on the contrary, the validity of their approach remains restricted to the fields much higher than B_{c2} , which is defined through $\tilde{B}_{c2} = \Phi_0/2\pi\xi^2$. Due to the symmetry of ξ with respect to T_c , the \tilde{B}_{c2} line in Fig. 3 (dashed line) is symmetric to the experimentally determined line for B_{c2} . We have taken the criterion of $3\tilde{B}_{c2}$ as the minimum field for the validity of the high field approximation. The dotted line at $T > T_c$ in Fig. 3 marks this boundary. In Fig. 4, the high field regime includes the fluctuation conductivity for $T < T_c$, and the high field sections of the curves at $T > T_c$. The scaling of σ_f according to the theory of Ullah and Dorsey is shown in Fig. 5. We note that it is common to take T_c as a fit parameter in scaling the experimental data.⁸⁻¹⁰ Here, T_c is predetermined from the B_{c2} line in Fig. 3, and the scaling in Fig. 5 is obtained with no free parameters. The consistency with three-dimensional (3D) scaling law [Fig. 5(a)] is obvious while 2D scaling law [Fig.

5(b)] is less satisfactory. 3D scaling near T_c was also observed in magnetization measurements.^{8,9} This feature is expected in layered copper oxide superconductors when, near T_c , the coherence length along the c axis exceeds the spacing of the layers so that discreteness may be replaced by continuum.

We have also examined whether our data on the fluctuation conductivity would scale according to the 3D XY model of Salamon *et al.*¹⁹ It was not possible to obtain a collapse of all the scaled data points onto a single curve, even with a free adjustment of T_c . We also note that recent measurements of the penetration depth by Kamal *et al.*²⁰ have shown 3D XY critical behavior in zero field in a temperature interval of 10 K below T_c , which is much wider than that previously observed at high magnetic fields.¹⁹ In contrast, our observations restrict the fluctuations dominated range in zero magnetic field to less than 1 K below T_c , and to progressively larger ranges at high magnetic fields (see Fig. 2). We believe that further research, including careful variation of oxygen content, is needed to elucidate the reasons for the observed differences.

In conclusion, we have shown that microwave magnetoresistance in high- T_c superconductors can be a powerful technique for the study of superconducting fluctuations. The experimental curves can be analyzed in such a way that mean-field T_c can be determined unambiguously, and the scaling of the fluctuation conductivity can then be probed without free parameters. Our results on $\text{YBa}_2\text{Cu}_3\text{O}_{7-\delta}$ single crystal show that the theory of Ullah and Dorsey in high fields yields a satisfactory 3D scaling.

¹J. P. Carini *et al.*, Phys. Rev. B **37**, 9726 (1988).

²D. L. Rubin *et al.*, Phys. Rev. B **38**, 6538 (1988).

³L. Drabeck *et al.*, Phys. Rev. B **40**, 7350 (1989).

⁴K. Holczer *et al.*, Phys. Rev. Lett. **67**, 152 (1991).

⁵D. A. Bonn *et al.*, Phys. Rev. Lett. **68**, 2390 (1992).

⁶T. Shibauchi *et al.*, Physica C **203**, 315 (1992).

⁷S. E. Inderhees *et al.*, Phys. Rev. Lett. **66**, 232 (1991).

⁸U. Welp *et al.*, Phys. Rev. Lett. **67**, 3180 (1991).

⁹Q. Li *et al.*, Phys. Rev. B **46**, 5857 (1992).

¹⁰R. Hopfengärtner, B. Hensel, and G. Saeman-Ischenko, Phys. Rev. B **44**, 741 (1991).

¹¹M. L. Horbach and W. van Saarloos, Phys. Rev. B **46**, 432 (1992).

¹²M. Požek, I. Ukrainczyk, B. Rakvin, and A. Dulčić, Europhys. Lett. **16**, 683 (1991).

¹³The same piece of single crystal was first annealed in oxygen for only two weeks, and the microwave surface resistance was measured. The observed slope ($d\rho_n/dT$) was half of that reported presently after the crystal was annealed in oxygen for additional two weeks.

¹⁴D. Achkir *et al.*, Phys. Rev. B **48**, 13 184 (1993).

¹⁵J. Owliaei, S. Sridhar, and J. Talvacchio, Phys. Rev. Lett. **69**, 3366 (1992).

¹⁶A. Dulčić and M. Požek, Physica C **218**, 449 (1993).

¹⁷V. A. Berezin *et al.*, Phys. Rev. B **49**, 4331 (1994).

¹⁸S. Ullah and A. T. Dorsey, Phys. Rev. B **44**, 262 (1991).

¹⁹M. B. Salamon *et al.*, Phys. Rev. B **47**, 5520 (1993).

²⁰S. Kamal *et al.*, Phys. Rev. Lett. **73**, 1845 (1994).